

MEASUREMENT OF DENSITY TURBULENCE AND BROADBAND MAGNETIC FLUCTUATIONS
ON ASDEX

G. Dodel, E. Holzhauser, and J. Massig

Institut für Plasmaforschung, Universität Stuttgart, Fed. Rep. of Germany

J. Gernhardt, ASDEX-, ICRH-, LH-, NI-, and Pellet-Teams,

Max-Planck-Institut für Plasmaphysik, EURATOM-Association, Garching, FRG

Broadband fluctuations of the electron density and the magnetic field were observed under various operational conditions of ASDEX using a laser scattering experiment and Mirnov coils, respectively. The aim of such measurements is to reveal the physical nature of the fluctuations and their possible correlation to anomalous particle and energy transport properties.

1. Density fluctuations.

The scattering system using a 119 μm CH_3OH laser and homodyne detection is described in more detail elsewhere [1]. It is able to detect density fluctuations propagating in nearly vertical direction. Movable optics allow a stepwise k_{\perp} -scan within one tokamak discharge and a shot to shot spatial scan of a large part of the poloidal plane. The spatial resolution is ± 1 cm in the vertical direction and depends on k_{\perp} in the horizontal direction. For $k_{\perp} \leq 10 \text{ cm}^{-1}$, where the dominant part of the fluctuation spectrum is found, the measurements are chord-averaged. The k_{\perp} resolution is $\pm 3.2 \text{ cm}^{-1}$.

The temporal development of the fluctuation spectra could be monitored with fixed frequency channels. Plateau phases of the tokamak discharge allowed frequency spectra to be scanned continuously with a spectrum analyzer.

a) Ohmic heating

In the range $5 \text{ cm}^{-1} \leq k_{\perp} \leq 20 \text{ cm}^{-1}$ the frequency integrated scattered power $P_S(k_{\perp})$ decreases as $k_{\perp}^{-\alpha}$, where $\alpha \approx 4$. The frequency power spectra $P_S(f)$ for fixed k_{\perp} are broadband. A frequency roll-off on the order of 6 dB/100 kHz is observed above 100 kHz. The root of the frequency integrated power $P_S^{1/2}$ scales linearly with the mean electron density \bar{n}_e in the range $5 \times 10^{12} \text{ cm}^{-3} \leq \bar{n}_e \leq 5 \times 10^{13} \text{ cm}^{-3}$ (Fig. 1). This corresponds to a nearly constant relative fluctuation level \tilde{n}_e/n_e .

b) Neutral beam injection (NI) heating.

L-discharges: With neutral injection the frequency spectra $P_S(f)$ become broader with increasing heating power. In the majority of L-discharges the frequency integrated scattered power increased above the ohmic level during neutral injection as illustrated in Fig. 2. A maximum enhancement by a factor of ~ 9 was observed with co-injection. In a series of counter-injection shots at constant n_e the increase of P_S with P_{NI} was approximately linear for P_{NI} up to 3.5 MW.

H-discharges: The temporal development of the fluctuation spectra at the transition from the L-phase into a burstfree H-phase is shown in Fig. 3. A comparison of the low- and high frequency channels shows a broadening of

the spectrum and a decrease in the frequency integrated scattered power although the line density \bar{n}_e increases. A similar observation was reported in [3]. There is evidence for a shift in the k_{\perp} spectrum towards longer fluctuation wavelengths. In contrast to the sharp L-H transition indicated by the D_{α} -monitor in the divertor chamber the frequency integrated scattered power changes on a much longer time scale, which corresponds to the global change in the density and temperature profiles.

In normal H-discharges with edge-localized modes the behaviour of the scattering signals is irregular.

c) Ion cyclotron resonance heating.

The scattering signals increase above the ohmic level for $k_{\perp} \leq 5 \text{ cm}^{-1}$ as reported also by [4]. Density fluctuations with $k_{\perp} \leq 7.5 \text{ cm}^{-1}$ are observed at the heating frequency (33.5 and 67 MHz).

d) Lower hybrid heating and current drive.

No significant changes in the low-frequency density fluctuations with respect to the ohmic phase are found.

e) Sawtooth activity.

Precursors to the sawtooth crash in the soft X-ray signals are observed in the frequency range $> 500 \text{ kHz}$. There is experimental evidence that they are localized only inside the $q=1$ surface. Increased fluctuations below 500 kHz are also found outside the $q=1$ surface, but only after the sawtooth crash [1].

f) Pellet injection.

An increase of the scattered signal is observed which starts with the ablation of the pellet. For single pellets the scattered signal decreases with the relaxation of the radial density profile [1].

In order to obtain a conclusive picture of the nature of the density turbulence and possible correlations to anomalous transport properties the measurements will be extended to wavenumbers below 5 cm^{-1} .

2. Magnetic fluctuations.

Mirnov coils in the limiter shadow of ASDEX were used to demonstrate the existence of broadband magnetic fluctuations with radial and poloidal components. Above about 70 kHz the temporal evolution of these spectra is distinctly different from the coherent Mirnov oscillations and their harmonics at lower frequencies.

If we assume that the field due to current disturbances decays like a vacuum field outside the plasma boundary in a cylindrical geometry, we can estimate the dominant poloidal mode number. For L-mode discharges with NI the plasma position, and thus the distance to the Mirnov coil, were varied. From the observed radial decay length a value of $m \geq 10$ is deduced. Typical fluctuation levels at the probe position were $B_r/B_t = 10^{-5}$. From 70 kHz to 200 kHz the spectral power density drops by a factor of 10. No qualitative

difference was seen in the temporal development of the radial and poloidal field components.

a) Ohmic heating.

The power spectra of the magnetic fluctuations are not correlated with those of the density fluctuations. During a linear density ramp the signal power of the magnetic fluctuations decreased slightly in contrast to the density fluctuations (Fig. 1).

b) Additional heating (L-phase).

The signal power increases for all types of heating used and the frequency spectrum broadens. An example recorded during an L-discharge with NI is given in Fig. 2.

c) Additional heating (H-phase).

After the transition into a burstfree H-phase the signal power begins to increase again as shown in Fig.4. When edge localized modes, indicated by spikes in the D_{α} signal, appear, the magnetic fluctuation signal is strongly modulated.

d) Sawtooth activity.

In the presence of sawteeth (during additional heating) the fluctuations suddenly increase at the time of the sawtooth crash, similarly to the D_{α} -signal observed in the divertor chamber [2].

e) Influence of boundary layer.

The magnetic probe signals seem to depend on conditions in the plasma boundary layer, as can be seen in the case of gas puffing or the modulation by edge localized modes.

3. Summary.

Significant but distinct changes in the fluctuation spectra have been observed in the various operating regimes of ASDEX. When comparing the behaviour of the density and magnetic field fluctuations it should be kept in mind that the two diagnostics have different spatial weighting functions, defined by the scattering volume in the former case and by the distance from the probe and the mode number m in the latter case. Further experiments will be needed before a comparison with proposed theoretical models for the fluctuations and their propagation mechanism inside the plasma can be made.

References

- [1] Dodel, G., Holzhauser, E., Massig, J., Vogel, T., Ignacz, P., ASDEX-, ICRH-, LH-, NI-, and Pellet-Teams, in "Basic and Advanced Diagnostic Techniques for Fusion Plasmas", Varenna (Italy), Sept. 1986, Vol. II, p.589 DOC. CEC EUR-10797 EN.
- [2] IPP Garching, Annual Report 1986, p. 15
- [3] Crowley, T., and Mazzucato, E., Nucl. Fusion 25, (1985), 507
- [4] TFR Group, and Truc, A., Plasma Phys., 27, (1985), 1057

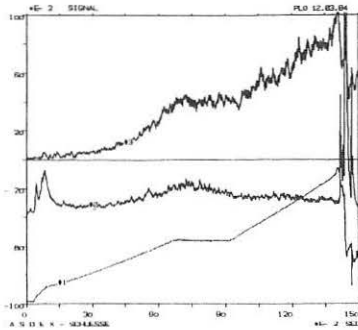


Fig.1 Density- and magnetic fluctuation signals in a shot with density ramping. From top to bottom: rms-scattering signal $P_S^{1/2}$; $f = 100 \pm 15$ kHz; $k_{\perp} = 7.5$ cm $^{-1}$. Magnetic signal power; $f = 100 \pm 15$ kHz. Line electron density \bar{n}_e . (Full time interval of abscissa: 1.5 s)

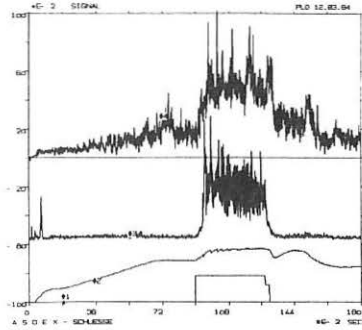


Fig.2 Density- and magnetic fluctuation signals in a L-discharge with NI. From top to bottom: Scattering signal P_{Si} ; $f = 60$ kHz - 1600 kHz; $k_{\perp} = 7.5$ cm $^{-1}$. Magnetic signal power; $f = 100 \pm 15$ kHz. Line electron density \bar{n}_e . NI beam monitor; $P_{NI} = 2.64$ MW. (Full time interval of abscissa: 1.8 s)

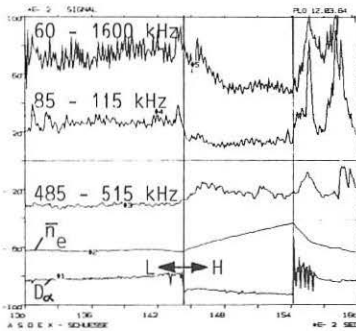


Fig.3 Density fluctuation signals in different frequency channels at the transition from an L-phase into a burstfree H-phase. $k_{\perp} = 5$ cm $^{-1}$. Lower traces: line electron density \bar{n}_e and D_{α} -monitor. (Full time interval of abscissa: 300 ms).

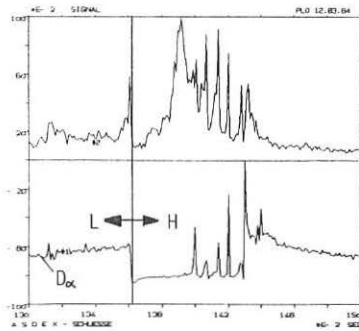


Fig.4 Magnetic fluctuation signal power at the transition from an L-phase into a burstfree H-phase followed by edge localized modes; $f = 100 \pm 15$ kHz. Lower trace: D_{α} -monitor. (Full time interval of abscissa: 200 ms).